

**SUPPORTING INFORMATION FOR:**

**Two-Photon Lithography in Visible and NIR Ranges  
Using Multibranch-based Sensitizers  
For Efficient Acid Generation**

Ming Jin<sup>\*,a</sup>, Jianchao Xie <sup>a</sup>, Jean-Pierre Malval<sup>\*,b</sup>, Arnaud Spangenberg<sup>b</sup>, Olivier Soppera <sup>b</sup>, Davy-Louis Versace <sup>c</sup>, Tiffanie Leclerc <sup>b</sup>, Haiyan Pan <sup>a</sup>, Decheng Wan <sup>a</sup>, Hongting Pu<sup>a</sup>, Patrice Baldeck <sup>d</sup>, Olivier Poizat<sup>e</sup> and Stephan Knopf <sup>b</sup>

<sup>a</sup> School of Materials Science and Engineering, Tongji University, Shanghai 201804, P.R. China.

<sup>b</sup> Institut de Science des Matériaux de Mulhouse, UMR CNRS 7361, Université de Haute-Alsace, 15 rue Jean Starcky, 68057 Mulhouse, France.

<sup>c</sup> Institut de Chimie et des Matériaux Paris-Est, UMR 7182, 2-8 rue Henri Dunant, 94320 Thiais. Université Paris-Est Créteil Val de Marne, France.

<sup>d</sup> Laboratoire de Spectrométrie Physique, UMR CNRS 5588. Université Joseph Fourier, 38402 Saint Martin d'Hères, France.

<sup>e</sup> Laboratoire de Spectrochimie Infrarouge et Raman, UMR CNRS 8516. Université des Sciences et Technologies de Lille. 59655 Villeneuve d'Ascq Cedex

Contact: [mingjin@tongji.edu.cn](mailto:mingjin@tongji.edu.cn) or [jean-pierre.malval@uha.fr](mailto:jean-pierre.malval@uha.fr)

**CONTENTS**

- Figure S1.** 2PEF spectra of **1** ( $9 \times 10^{-5}$  M in ACN,  $\lambda_{\text{exc}}$ : 760 nm) using two distinctive detection configurations. **A.** The excitation focal point is located in the middle of the cell (1 cm quartz cuvette); **B.** The excitation focal point is positioned very close to the detection window. In both cases, the 1PEF spectrum was measured using the classical method with a spectrofluorimeter ( $10^{-6}$  M in ACN,  $\lambda_{\text{exc}}$ : 370 nm).
- Figure S2.** Evolution of the absorption spectrum of **1** ( $2.4 \times 10^{-4}$  M in degassed ACN) in presence of  $\text{Ph}_2\text{I}^+, \text{PF}_6^-$  ( $1.5 \times 10^{-3}$  M) during irradiation at 365 nm. Rhodamine B base ( $1 \times 10^{-5}$  M) is added as acid indicator.
- Figure S3.** Representation of frontier molecular orbitals involved in the lowest energy electronic transitions of the chromophores.
- Figure S4.** Solvatochromic plots of Stokes shift for the chromophores.
- Figure S5.** Time fluorescence decays of the chromophores recorded at their respective  $\lambda_{\text{fluo}}^{\text{MAX}}$ ; instrumental response function (IRF). Residual graphs relative to single- or bi-exponential fits. (solvent: Hexane).
- Figure S6.** Plots of  $\log I_{\text{fluo}}$  ( $\lambda_{\text{fluo}}$ : 475 nm) vs.  $\log[\text{excitation power}]$  at 500 nm for **3**. (THF, c:  $1.5 \times 10^{-4}$  M).
- Figure S7.** Fluorescence spectra of **1** in dichloromethane upon addition of **PAG**. Inset: Stern-Volmer plots as observed by steady state fluorescence intensities and emission lifetimes.
- Figure S8.** Comparison of the conversion vs. time curves for cationic photopolymerization of diepoxide films under aerated and laminated conditions. (resin: **PAG** (1.5 wt %) / **3** (0.15 wt %).  $\lambda_{\text{exc}}$ : 365 nm, Irradiance: 45 mW cm<sup>-2</sup>).

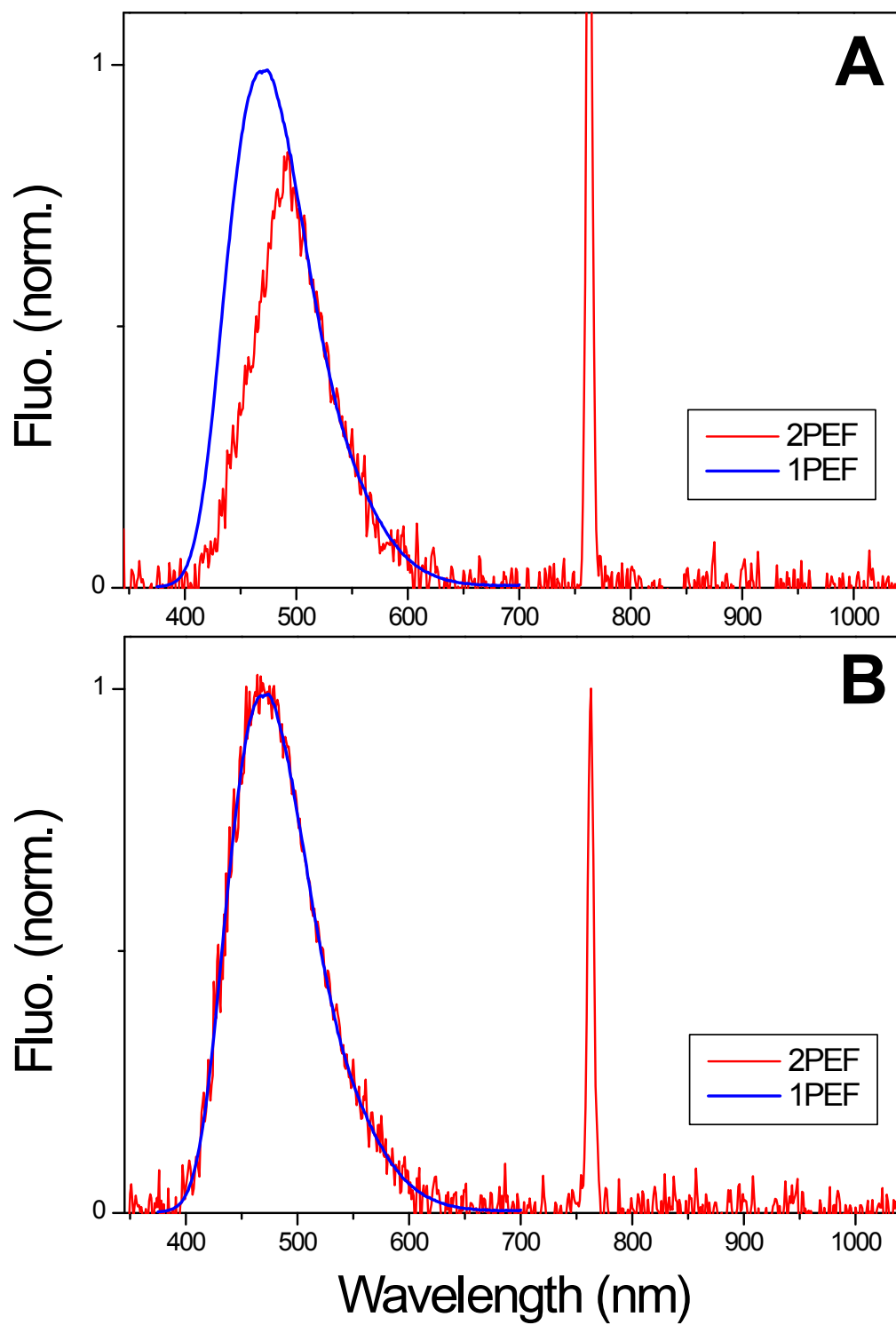


Figure S1.

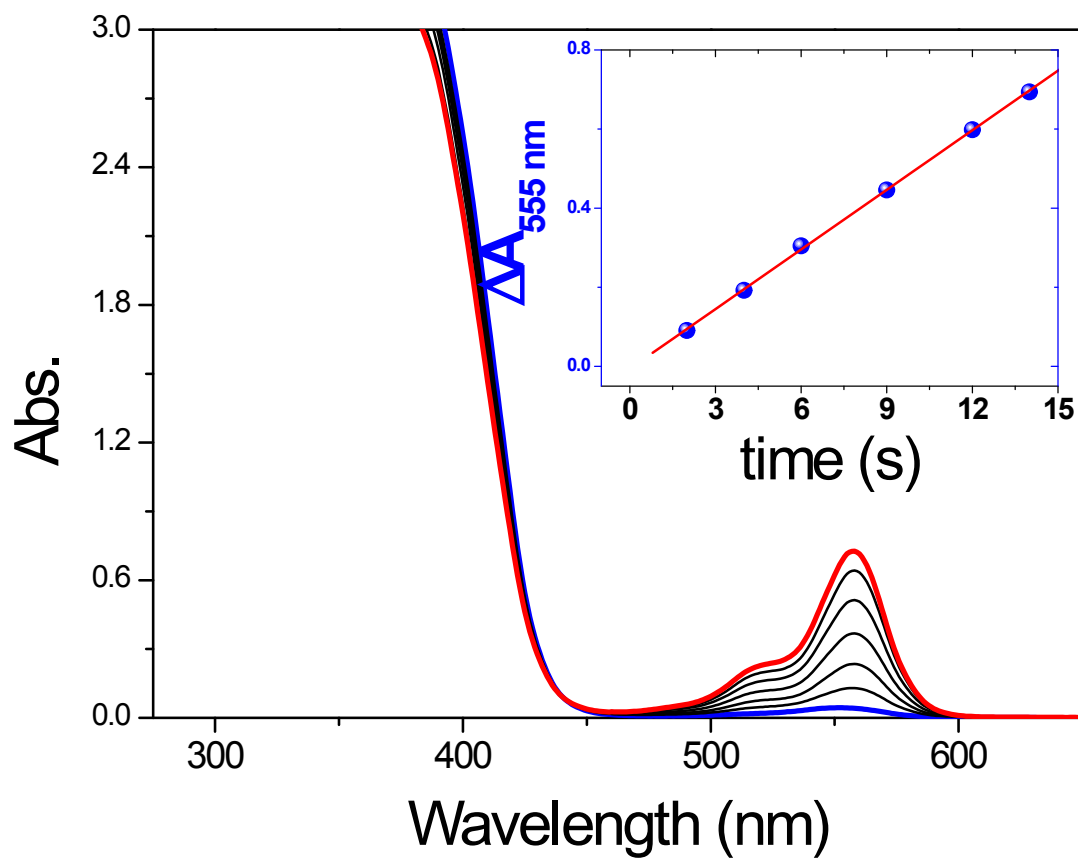


Figure S2.

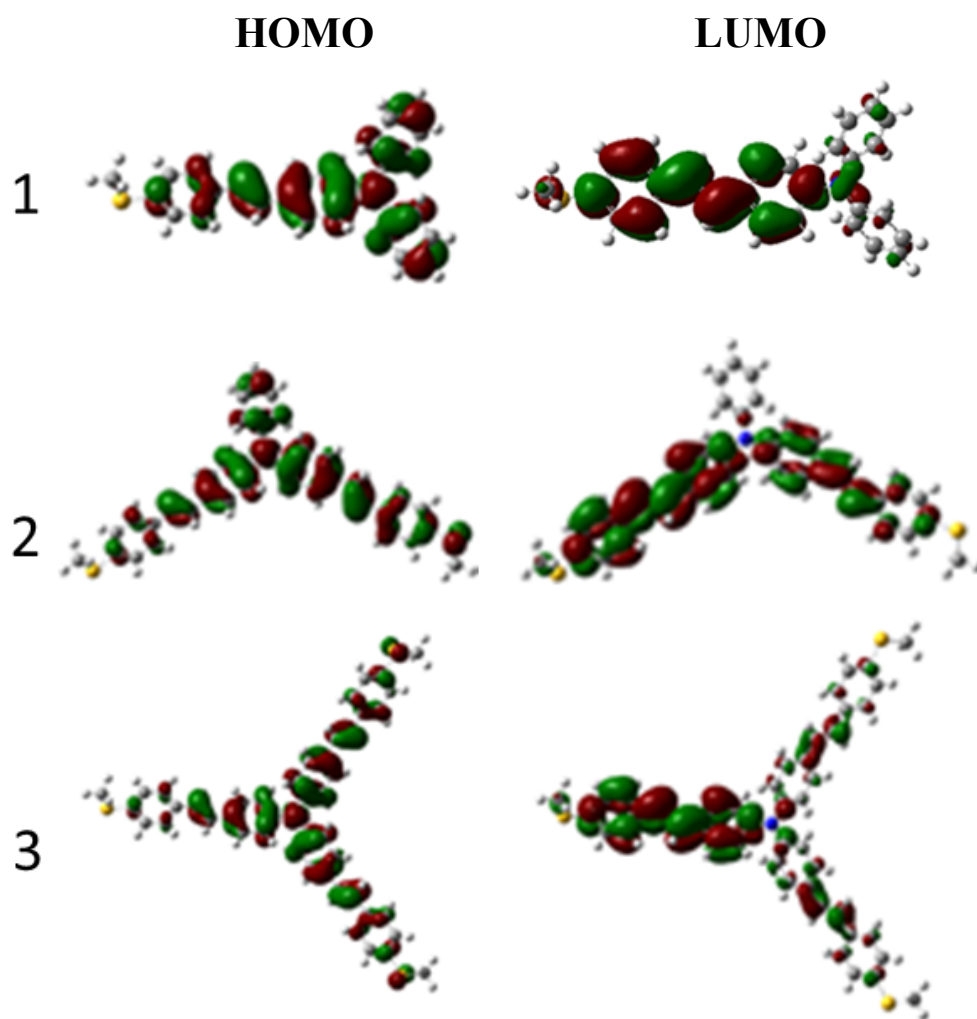


Figure S3.

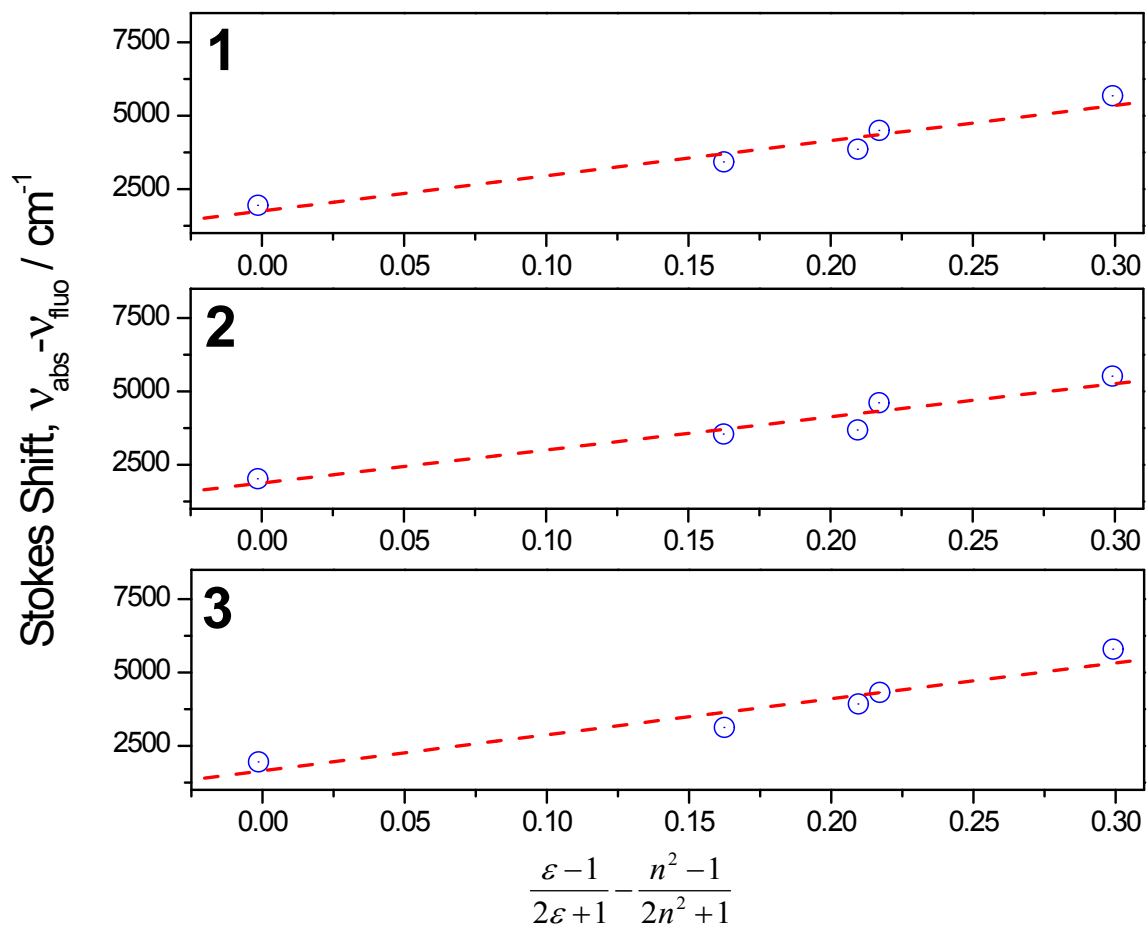


Figure S4.

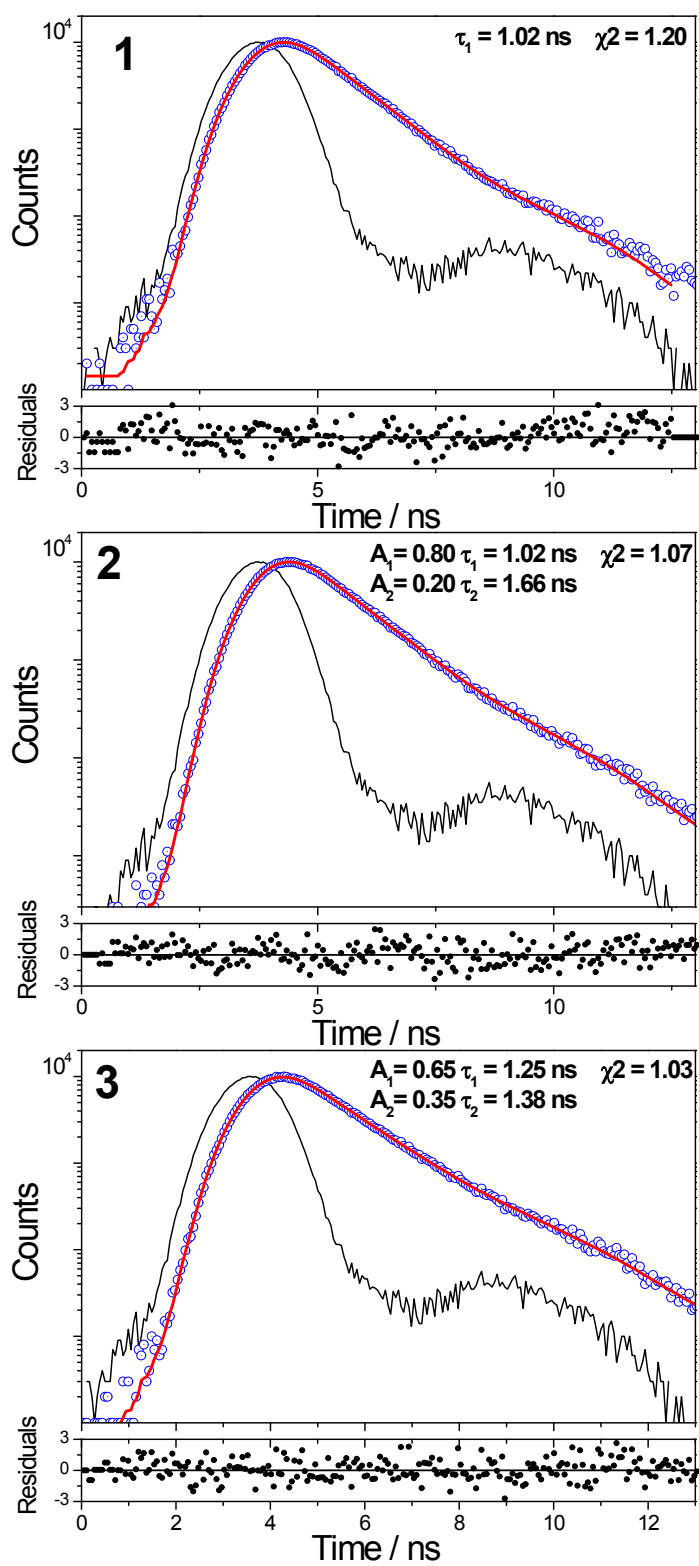


Figure S5.

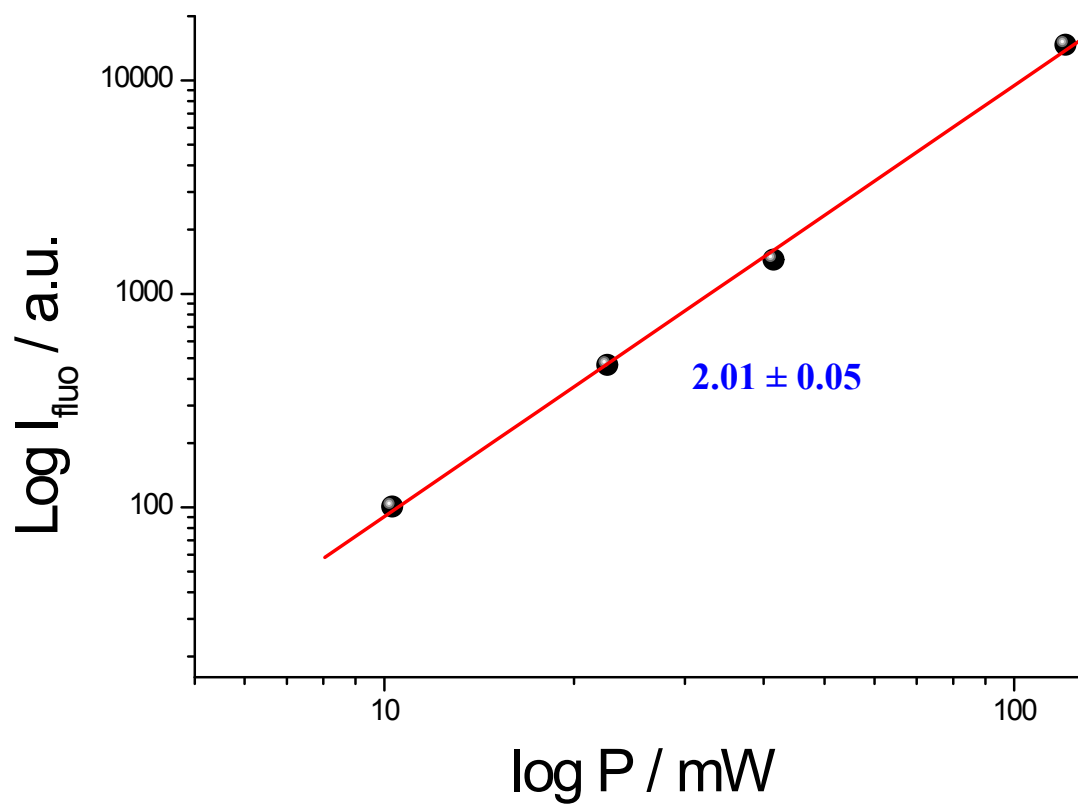


Figure S6.

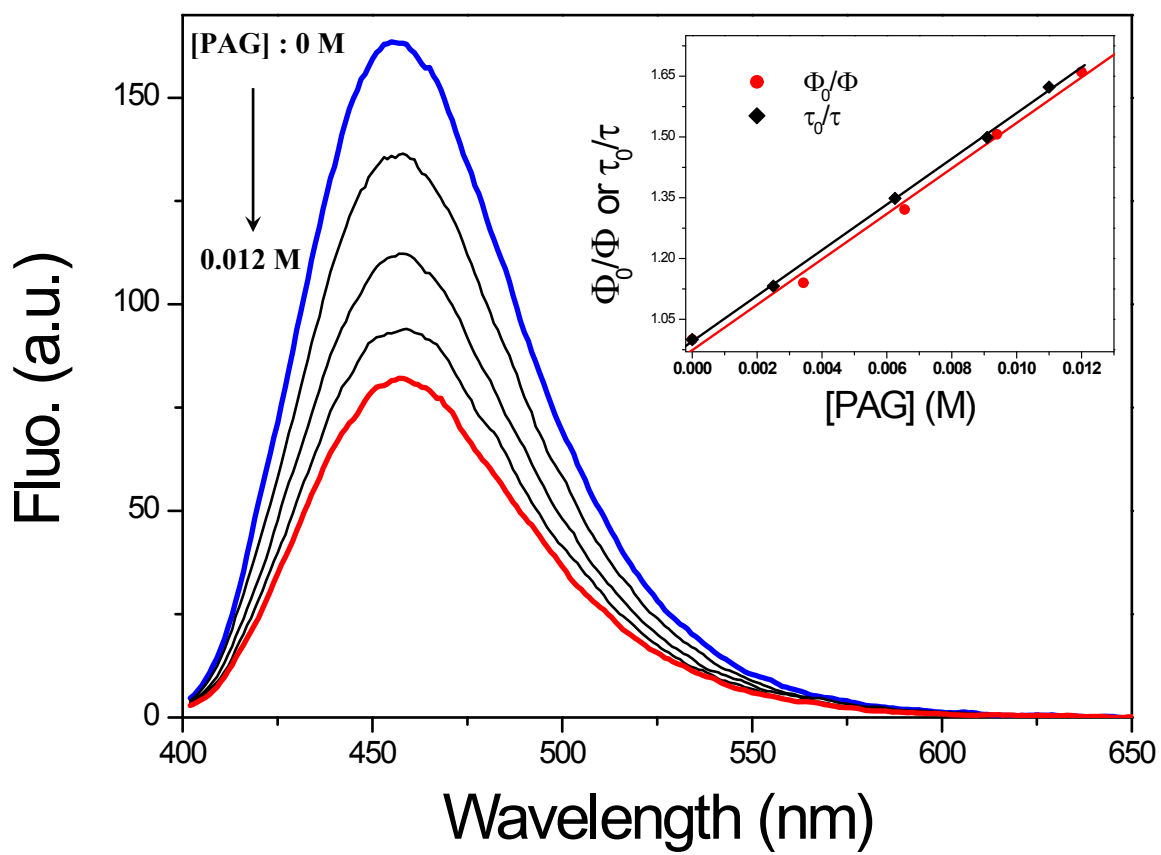


Figure S7.



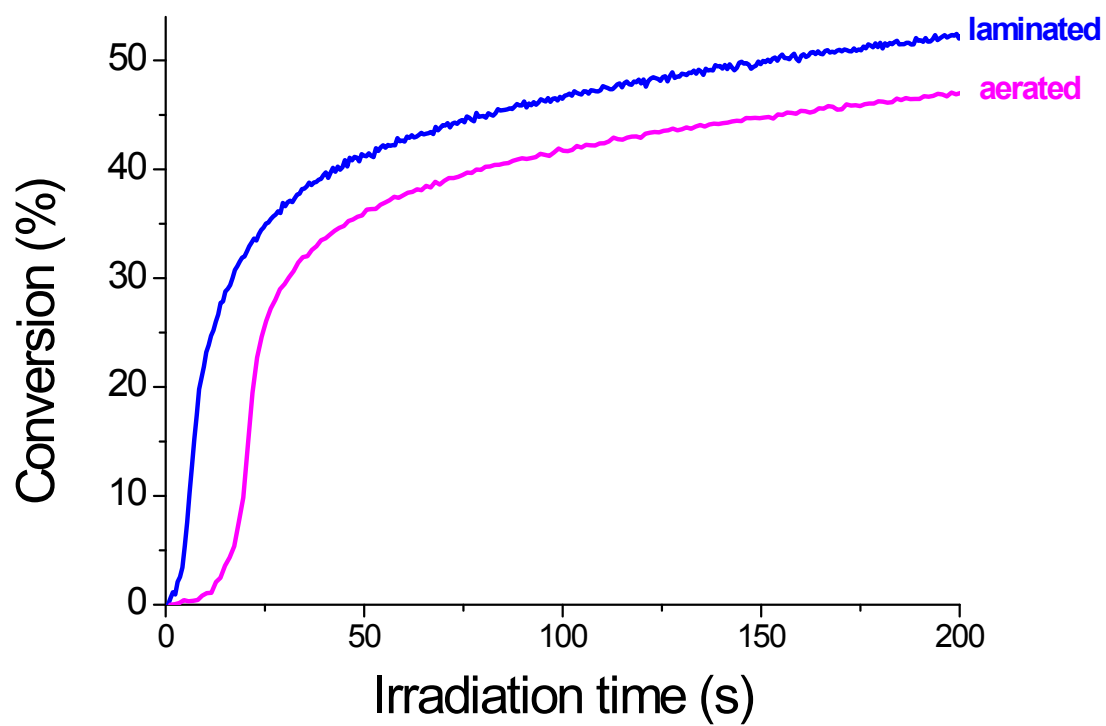


Figure S8.